JOURNALS OF CATALYSIS **159,** 394–400 (1996)
ARTICLE NO. 0102

A Kinetic Model for Alumina Sulfation

Anne Pieplu,* Odette Saur,* Jean-Claude Lavalley,*,[1] Michèle Pijolat,† and Olivier Legendre‡

*Laboratoire de Catalyse et Spectrochimie, URA CNRS 0414, ISMRA-Université, 6 Boulevard du Maréchal Juin, 14050 Caen Cédex, France; †Centre SPIN, Ecole des Mines, 58 Cours Fauriel, 42023 St Etienne Cédex-02, France; and ‡Rhône-Poulenc Recherche, Centre d'Aubervilliers, 52 Rue de la Haie Coq, 93308 Aubervilliers, France

Received May 24, 1995; revised October 16, 1995; accepted October 31, 1995

SO_2 adsorption on alumina and sulfation with $SO_2 + O_2$ have been investigated by IR spectroscopy and thermogravimetric measurements at temperatures quite similar to Claus process plant operating conditions (280–350°C). The sulfation was studied under various $P(SO_2)$ and $P(O_2)$ pressures. The results allow a kinetic model for alumina sulfation to be proposed. The elementary steps of the mechanism involve two types of surface site. The same site contributes to SO_2 adsorption as sulfite and to sulfate formation. Another catalytic site leads to oxygen dissociation. On pure alumina the number of this last site is very low. The model enables the weight gain due to the fixation of SO_2 and O_2 to be expressed as a function of time. Kinetic constants were calculated from various sulfation experiments and the theoretical expression so obtained fits the experimental curves.

INTRODUCTION

The modified Claus process has been used for many years to remove H_2S from gas effluents. A fraction of hydrogen sulfide (1/3) is converted into elemental sulfur in a thermal stage (1200°C) according to the reactions

$$H_2S + 3/2\,O_2 = SO_2 + H_2O \qquad [R1]$$

$$2H_2S + SO_2 = 3/n\,S_n + 2H_2O. \qquad [R2]$$

Nevertheless, the conversion of H_2S (reaction [R2]) is thermodynamically favored at lower temperatures and a catalytic stage is necessary. The most frequently employed catalyst is alumina. Its deactivation has often been studied. The importance of sulfation has been proved (1, 2). The formation of sulfate species not only affects the rate of this reaction [R2] but also influences the rate of COS and CS_2 hydrolysis (1, 3). COS and CS_2 are poisoning gases produced in Claus plants during the thermal stage when natural gas or refinery streams contain CO_2 and hydrocarbons.

Previous studies showed that sulfation could occur by SO_2 or H_2S oxidation (4). The modeling of alumina sulfation by oxidation of these sulfur compounds in Claus plant operating conditions (280–350°C) has not yet been studied. However, Nam and Gavalas (5) proposed a mechanism of alumina sulfation but at temperatures of 500–700°C. Comparing initial rates of adsorption and oxidative adsorption of SO_2, these authors suggested that SO_2 adsorption was the first step in the formation of sulfate species. Their results showed that adsorbed SO_2 was oxidized to surface sulfate which remained at the original SO_2 adsorption sites. Then they suggested a two-site mechanism with strong and weak adsorption sites.

The modeling of γ-alumina sulfation needs to be able to predict the amount of surface sulfate species which poison Claus catalyst according to flue gas composition. Therefore we tried to find a kinetic model of γ-alumina sulfation in the presence of $SO_2 + O_2$.

Many FT-IR and EPR spectroscopic studies related to SO_2 adsorption on γ-alumina at room temperature have led to the identification of several surface species. In 1978, Chang (6) characterized two species formed at room temperature by IR bands at 1060 cm^{-1} and 1326–1140 cm^{-1}. He assigned the first band to strongly adsorbed SO_3^{2-} species. Karge and Dalla Lana (7) showed by selective poisoning that these species, called sulfite species, were chemisorbed on O^{2-} basic sites. They also revealed that IR bands at 1330–1150 cm^{-1} came from species formed by SO_2 adsorption, slightly bonded to Lewis acid sites. Moreover, Lavalley *et al.* (8) suggested the occurrence of bisulfite species resulting from interaction between SO_2 and the most basic OH groups of alumina.

More recently, Datta *et al.* (9) presented and characterized by IR and EPR spectroscopy five adsorbed species at room temperature on more or less dehydroxylated alumina, summarizing and supplementing the previous works.

Unlike SO_2 adsorption, few authors have studied the nature of species formed during alumina sulfation in the presence of SO_2 and O_2. After evacuation at 450°C of alumina samples sulfated by $SO_2 + O_2$ gas or by impregnation with $(NH_4)_2SO_4$, the same surface species appeared and its infrared spectrum was quite different to the bulk aluminium sulfate spectrum (10, 11). The spectrum of this surface sulfate species showed a sharp IR band near 1380 cm^{-1} and a

[1] To whom correspondence should be addressed.

0021-9517/96 $18.00

broad one near 1045 cm^{-1}. The first had been assigned by isotopic exchanges to a ν(S=O) vibration and the second to ν(S–O) vibrations. These species were thermally stable up to 600°C. The IR spectrum modification in the presence of steam at room temperature showed the sensitivity of this structure to water.

We have used these IR results and thermogravimetric measurements to establish a mechanism of alumina sulfation by $SO_2 + O_2$.

EXPERIMENTAL

Alumina (Condea) was a powdered form of γ-alumina obtained from Rhône-Poulenc which had been calcined for 4 h at 600°C. Its sodium content was low (<25 ppm). The BET surface area was 215 $m^2\ g^{-1}$ and the porosity was 0.42 $cm^3\ g^{-1}$.

For IR study, the powder was pressed at 40 MPa into self-supporting disks of approximately 10 mg cm^{-2}. The wafers were activated by heating under vacuum for about 2 h. IR spectra were recorded at room temperature using a MX-1 Nicolet spectrometer.

A standard McBain thermobalance, working under static conditions, was used to measure the weight changes of the samples during adsorption and desorption. Typically 400 mg of broken disks pressed at 40 MPa were placed in a quartz sample pan. Samples were evacuated first at room temperature for 7.5 h ($P<10^{-3}$ Pa) and then the temperature was gradually increased to 450°C (1°/min). The temperature remained at 450°C for 15 h. In these conditions, the mass loss was about 13% and was ascribed to CO_2 and H_2O elimination. After activation, temperature was decreased before gas introduction.

RESULTS

a. SO_2 Adsorption on γ-Alumina

Figure 1 presents the variation of the sample weight observed by gravimetry during SO_2 adsorption at 250 and 350°C ($P(SO_2) = 0.8$ kPa). The adsorption phenomenon seems to occur in a similar way at the two temperatures. The weight increased very rapidly during the first hour and then varied more slowly. At 350°C, the amount of adsorbed SO_2 after 24 h of gas exposure was about 2 μmol m^{-2} or 1.2 molecule per 100 $Å^2$, 91% being adsorbed during the first hour. At 250°C, the amount of adsorbed SO_2 after 5 h was about 2.2 μmol m^{-2}. At 500°C Nam and Gavalas (5) obtained similar curves and measured 0.67 μmol m^{-2} of SO_2 adsorbed under 0.8 kPa. We also studied the SO_2 desorption and obtained similar results to those reported in the literature (5).

. The SO_2 adsorption isotherm on γ-alumina at temperatures close to 350°C (Fig. 2) is comparable with those obtained by Chang (6) and Nam and Gavalas (5) at other temperatures on other types of alumina. These works led to the conclusion that SO_2 adsorption occurs on a restricted number of sites.

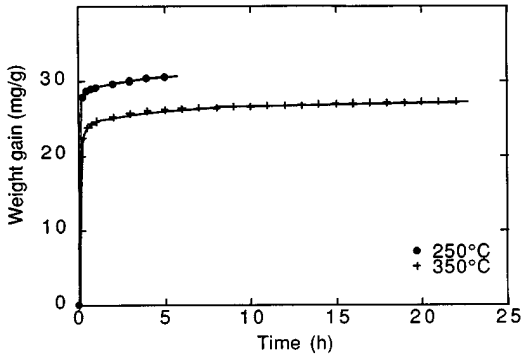

FIG. 1. SO_2 adsorption on alumina at 250 and 350°C. Variation of the weight of the sample versus time.

b. Alumina Sulfation with $SO_2 + O_2$

Gravimetric results. For the study of alumina sulfation by $SO_2 + O_2$, all experiments were carried out at 350°C. Two series of results were obtained according to the following pressure conditions: $P(SO_2) = 0.8$ kPa and $0.2 < P(O_2) < 15$ kPa or $P(O_2) = 3.2$ kPa, and $0.8 < P(SO_2) < 20$ kPa. Comparison of the curves obtained during SO_2 adsorption with those obtained during $SO_2 + O_2$ adsorption showed that the latter could be interpreted as the result of two processes, (i) SO_2 adsorption, which essentially gives a fast and important weight increase during the very first minutes, and (ii) oxidation of SO_2, which leads to a linear variation of the sample mass with time after about 5 h of gas exposure (Fig. 3), and we denote its slope as k.

In some experiments O_2 was introduced after SO_2 adsorption. The curves clearly showed a weight increase after O_2 addition and a more important weight gain when comparing to pure SO_2 adsorption.

Consequently, after about 5 h, when the steady state was reached, the linear part of the weight increase curve

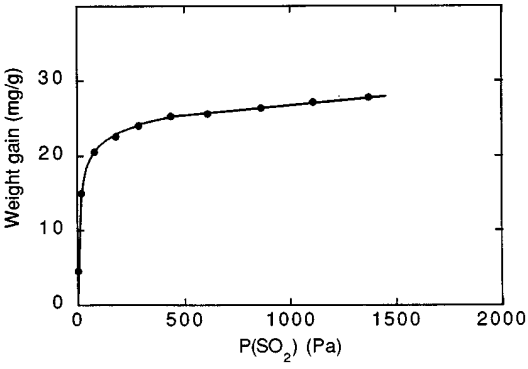

FIG. 2. Adsorption isotherm of SO_2 at 350°C.

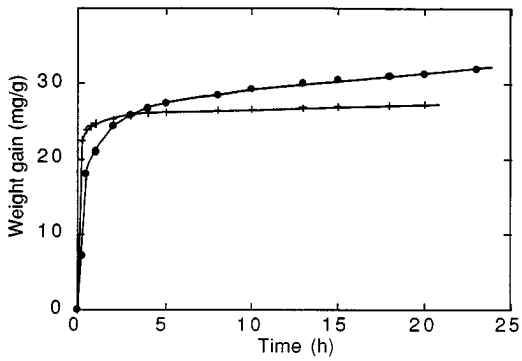

FIG. 3. Variation of the sample weight versus time. • Sample treated by $SO_2 + O_2$ at 350°C ($P(SO_2) = 0.8$ kPa; $P(O_2) = 10.8$ kPa); + Sample exposed to SO_2 ($P(SO_2) = 0.8$ kPa).

(Fig. 3) during $SO_2 + O_2$ exposure could represent the rate of sulfation. Figure 4 shows that this linear part varies with $P(SO_2)^{1.0}$ and $P(O_2)^{0.5}$. An increase in $P(O_2)$ leads to an increase in the slope k over the whole studied pressure range (0.2 to 15 kPa). A similar increase was observed when $P(SO_2)$ increased from 0.2 to 8 kPa; however, if $P(SO_2)$ was up to 8 kPa, the slope was practically constant.

IR study. The sulfated alumina samples obtained under $SO_2 + O_2$ treatment were studied by IR spectroscopy. In Fig. 5, the spectrum of a sulfated sample is reported. It shows, after subtracting Al_2O_3 absorbance (Fig. 5b), two IR bands near 1380 and 1040 cm^{-1} which were assigned to a surface sulfate species. An IR method for the determination of the amount of surface sulfate species was defined (10) using the 1380 cm^{-1} IR band. The measurement of the integrated absorbance of this band enables us to determine the amount of these species since the area of this band is proportional to the amount of sulfate ions adsorbed at the surface of the samples. However, this method has limits:

(i) The IR band near 1380 cm^{-1} is clearly observed if the sample is well dehydroxylated. The disks must be heated under vacuum for 2 h at 450°C.

TABLE 1

Comparison of IR and Ionic Chromatographic Results

	IR sulfate dosage (μmol g^{-1})	Ionic chromatography (μmol g^{-1})
Sample 1	170	173
Sample 2	400	421

(ii) If the amount of sulfate species is too large, the band absorbance reaches to 2 and quantitative measurements are impossible. Dilution of sulfated alumina with pure alumina can be done but increases the uncertainty of measurement. Ion chromatography measurements confirm the IR results (Table 1).

The IR results allow us to calculate the increase of mass due to the formation of sulfate species after 24 h. Subtracting this calculated mass from the weight gain observed by gravimetry we obtain the amount of SO_2 remaining adsorbed but not oxidized. The amounts of adsorbed SO_2 and SO_3 are compared in Table 2. We also report the number of sites involved in the adsorption of these species. These sites are basic oxygen atoms of the dehydroxylated alumina surface.

DISCUSSION

a. SO_2 Adsorption

Assuming a single type of adsorption site and using the Langmuir hypothesis, the linearization of the SO_2 adsorption isotherm at 350°C allows us to calculate the maximum number of sites (2.04 μmol m^{-2}, i.e., 1.23 molecule nm^{-2}) and the equilibrium constant ($K = 2.4\,10^3$ with P° (the pressure unit) = 1 bar).

According to the literature (5, 7, 9) and from the study of desorption, two types of sites could be viewed leading

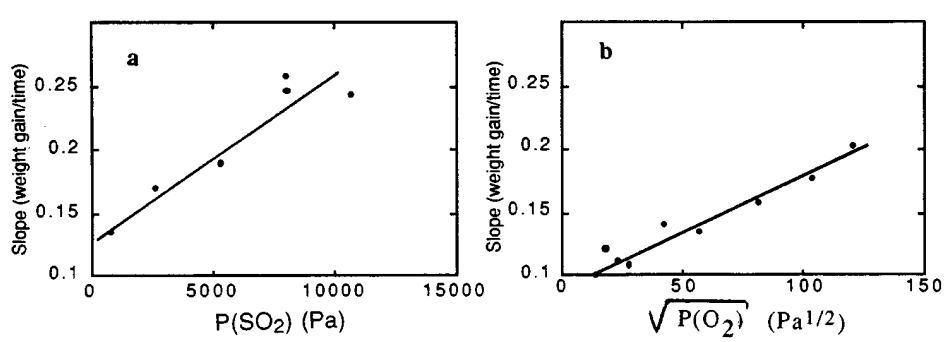

FIG. 4. Variation of the slope of the linear part of the sulfation curve (see Fig. 3) versus (a) $P(SO_2)$, $P(O_2)$ being constant, (b) $\sqrt{P(O_2)}$, $P(SO_2)$ being constant.

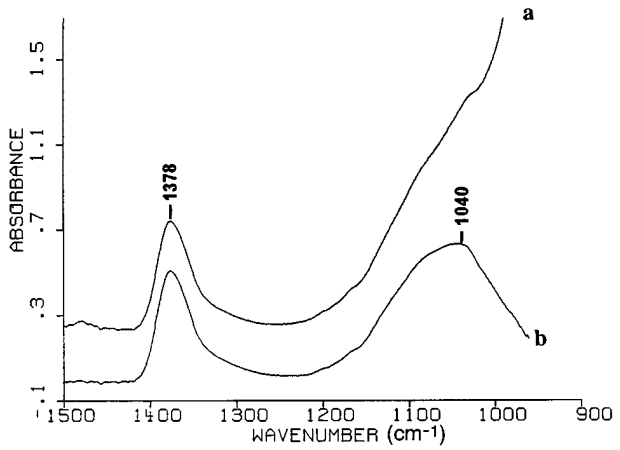

FIG. 5. Infrared spectra of (a) sulfated Al_2O_3 sample after evacuation at 450°C, and (b) sulfate species (the absorbance of Al_2O_3 had been subtracted).

to two types of adsorbed species, reversibly or irreversibly. Isotherms of adsorption could be interpreted assuming two different sites but such an attempt did not lead to coherent results at 350°C. Consequently, at 350°C, we later consider a single type of SO_2 adsorption site which could be a surface O^{2-} or OH^- in accordance with the hydroxylation degree of alumina.

b. Modeling of Alumina Sulfation ($SO_2 + O_2$)

Although aluminium sulfate is the thermodynamically stable state, we never observed this phase by IR (a bulk sulfate band expected near 1150 cm^{-1} was not observed) or by X-ray diffraction, but due to an experimentation time of only 24 h the extent of transformation never exceeded 4%. The studied transformation is nevertheless written as

$$Al_2O_3 + 3SO_2 + 3/2\,O_2 = Al_2(SO_4)_3.$$

For modeling, we make the assumption of non-steady-state kinetics. The diffusion from the gas phase to the sample is not taken into account since it can be assumed to be very fast; if it is not, the time scale is hours and the diffusion can still be ignored. The theoretical expressions of the sample weight versus time may take very different forms depending on the choice of the elementary steps. However, considering the experimental thermogravimetric curves, the rate of variation of the weight should be such as $(dm/dt)(t \to \infty) \ll (dm/dt)(t \to 0)$. Moreover, the model must lead to an expression which describes the experimental results obtained when $P(SO_2)$ and $P(O_2)$ are varied (Fig. 4).

In the proposed model, the SO_2 adsorption sites and those of SO_3 formed have to be the same. At 350°C, it was shown (4) by thermogravimetric studies of SO_2 adsorption on sulfated alumina that sulfite and sulfate species had the same type of adsorption site.

For modeling SO_2 oxidative adsorption, two types of processes are possible: either Rideal-type kinetics, with oxidative reaction taking place between adsorbed SO_2 species and gaseous or physically adsorbed O_2, or a Langmuir–Hinshelwood model, with oxidation of adsorbed SO_2 by an oxygen species resulting from dissociative oxygen chemisorption.

We never observed thermogravimetrically an increase of mass by oxygen adsorption. However, the amount of adsorbed oxygen may be too low to be detected. Since mass variation depends on $\sqrt{P(O_2)}$, the mechanism necessarily needs to include oxygen dissociation on the catalyst. It is difficult to specify on which type of sites the dissociation of O_2 molecules occurs. Oxygen dissociation needs electrons,

$$O_2 + 2V_O^{\cdot\cdot} + 4e' = 2O_O^x,$$

where Kröger's notation (12) is adopted. Oxygen vacancies are present on γ-Al_2O_3 but free electrons have never

TABLE 2

Amount of SO_2 and SO_3 Adsorbed on Alumina and Number of Adsorption Sites ($P(SO_2) = 800$ Pa)

$P(O_2)$ (Pa)	Total Δm^a (mg/g)	Δm due to sulfate[b] (mg/g)	Δm due to sulfate[b] (molec./nm^2)	Δm due to nonoxidized SO_2 (mg/g)	Δm due to nonoxidized SO_2 (molec./nm^2)	Total amount of SO_2 and SO_3 (molec./nm^2)
200	26.9	9.0	0.32	17.9	0.78	1.10
200	25.4	10.3	0.36	15.5	0.68	1.01
560	25.9	11.7	0.41	14.2	0.62	1.03
1820	27.0	11.2	0.39	16.6	0.73	1.12
3210	28.3	11.1	0.39	17.2	0.75	1.14
6690	30.3	22.1	0.77	8.2	0.36	1.13
14500	31.3	24.6	0.86	6.7	0.29	1.15

[a] Measured by thermogravimetry, after 24 h of $SO_2 + O_2$ treatment.
[b] Calculated from IR absorbance.

been noted. Notice that when the oxide is promoted by such metals as platinum, palladium, or vanadium, oxygen dissociation can be increased and thus sulfation favored.

The elementary steps of the proposed mechanism are noted as follows, again using Kröger's notation (12). (In this notation, $'$ refers to a net negative charge, x to a neutral defect, and $^\bullet$ to a positive charge. V is a vacancy, V''_D a tetrahedral Al vacancy, and $V^{\cdot\cdot}_O$ an oxygen vacancy and thus Al_2O_3 is denoted as $2Al^x_{Al}3O^x_O V''_D V^{\cdot\cdot}_O$.

$$SO_2 + O^x_{Osurf} \leftrightarrows SO^x_{3Osurf} \quad [S1]$$

$$2s + O_2 = 2O\text{-}s \quad [S2]$$

$$SO^x_{3Osurf} + O\text{-}s \rightarrow SO^x_{4Osurf} + s \quad [S3]$$

$$2Al^x_{Alsurf} + 3SO^x_{4Osurf} + 2Al^x_{Al} + 3O^x_O + V''_D + V^{\cdot\cdot}_O = Al_2(SO_4)_3 + 3O^x_{Osurf} + 2Al^x_{Alsurf} \quad [S4]$$

In this last step [S4], the sulfated surface layer of alumina contributes to the growth of the aluminium sulfate phase, while the structural elements of alumina which were just beneath the sulfated surface layer became surface oxygen and aluminium ions ready to be sulfated. In this mechanism, the nucleation of the sulfate phase was assumed to be instantaneous. Moreover, the extent of reactional area does not vary much since the last step was assumed to be always at equilibrium.

Multiplying the first step by 3, the second by 3/2, and the third by 3, the linear combination of steps [S1] to [S4] obtained leads to the studied reaction

$$Al_2O_3 + 3SO_2 + 3/2\,O_2 = Al_2(SO_4)_3.$$

Two types of sites are involved in this model. One of them, O^x_{Osurf} representing an oxygen ion of the alumina lattice, sits at the surface of the catalyst and exists in a large number. SO_2 is adsorbed on it in step [S1] as a sulfite-like species and thus is oxidized into sulfate (step [S3]). The other site written s (O_2 dissociation site) is a catalytic site restored after sulfate species formation (steps [S2] and [S3]). We suppose that this site only exists in a small number; this number is assumed to be constant because of regeneration during step [S3]. Then we have $[O^x_{Osurf}] = 1, [s] = a\,(a \ll 1)$, and [O-s] is constant.

The trial of several models led us to consider simultaneous SO_2 desorption (constant k'_1) and adsorption (constant k_1) to interpret the observation that $(dm/dt)(t \rightarrow \infty)$ was clearly lower than $(dm/dt)(t \rightarrow 0)$.

The weight gain is related to SO_2 and O_2 adsorptions (steps [S1] and [S2]); its rate can be written as

$$\frac{dm}{dt} = M(SO_2)v_1 + 2M(O)v_2 \quad [1]$$

with $M(SO_2) = 64\ g\ mol^{-1}$ and $M(O) = 16\ g\ mol^{-1}$. The step [S1] assumed to be elementary, v_1, is written

$$v_1 = k_1 P(SO_2) - k'_1[SO^x_{3Osurf}]. \quad [2]$$

Since the concentration of O-s site is constant, we write

$$\frac{d[O\text{–}s]}{dt} = 0 = 2v_2 - v_3. \quad [3]$$

Then $v_2 = v_3/2$. On the assumption that step [S3] is elementary and neglecting the rate of the reverse reaction in this step, we write

$$v_3 = k_3[SO^x_{3Osurf}][O\text{–}s]. \quad [4]$$

On the other hand, considering the steady-state hypothesis for O-s and s species, the step [S2] is at equilibrium and the mass action law applied to this equilibrium is written

$$K = \frac{[O\text{–}s]^2}{P(O_2)[s]^2}, \quad [5]$$

which leads to $[O\text{–}s] = a\sqrt{K\,P(O_2)}$ with $[s] = a$. We then obtain the following expression for *dm/dt*:

$$\frac{dm}{dt} = M(SO_2)(k_1 P(SO_2) - k'_1[SO^x_{3Osurf}]) + M(O)k_3[SO^x_{3Osurf}]a\sqrt{KP(O_2)}. \quad [6]$$

For the study of *dm/dt* limits, we may express $[SO^x_{3Osurf}]$ as a function of time. Because of steps [S1] and [S3], we write

$$\frac{d[SO^x_{3Osurf}]}{dt} = k_1 P(SO_2) - [SO^x_{3Osurf}]\left(k'_1 + k_3 a\sqrt{K\,P(O_2)}\right). \quad [7]$$

The solution of the first-order differential equation is

$$[SO^x_{3Osurf}] = \frac{k_1 P(SO_2)}{k'_1 + k_3 a\sqrt{K\,P(O_2)}}\left(1 - e^{-(k'_1 + k_3 a\sqrt{K\,P(O_2)})t}\right). \quad [8]$$

The $[SO^x_{3Osurf}]$and *dm/dt* limits are thus

$$[SO^x_{3Osurf}](t \rightarrow 0) = 0$$

and then

$$\frac{dm}{dt} = M(SO_2)(k_1 P(SO_2) \quad [9]$$

$$[SO^x_{3Osurf}](t \rightarrow \infty) = \frac{k_1 P(SO_2)}{k'_1 + k_3 a\sqrt{K\,P(O_2)}} \quad [10]$$

then

$$\frac{dm}{dt}(t \rightarrow \infty) = \frac{(M(SO_2) + M(O))P(SO_2)k_1 k_3 a\sqrt{K\,P(O_2)}}{(k'_1 + k_3 a\sqrt{K\,P(O_2)})}. \quad [11]$$

To satisfy the experimental observations, $(dm/dt)\,(t \to 0)$ may be higher than $(dm/dt)\,(t \to \infty)$ which leads to the condition

$$M(SO_2)k_1P(SO_2) > \frac{(M(SO_2)+M(O))P(SO_2)k_1k_3a\sqrt{KP(O_2)}}{k_1'+k_3a\sqrt{KP(O_2)}}, \quad [12]$$

which in turn gives

$$4k_1' > k_3a\sqrt{KP(O_2)}. \quad [13]$$

This relation is a priori possible and we shall check its validity later. On the other hand, if $P(O_2)$ is constant, the calculated expression for $(dm/dt)(t\to\infty)$ is a linear function of $P(SO_2)$. At least this was experimentally observed on condition that $P(SO_2)$ was lower than 8 kPa (Fig. 4a). If $P(SO_2)$ is constant, $(dm/dt)\,(t\to\infty)$ is a linear function of $\sqrt{P(O_2)}$ (as was experimentally observed, see Fig. 4b) only if we could neglect $k_3a\sqrt{KP(O_2)}$ besides k_1'. The condition $4k_1' > k_3a\sqrt{KP(O_2)}$ is then restricted to $k_1' > k_3a\sqrt{KP(O_2)}$. By integration of *dm/dt* (Eq. [6]) we obtain the expression for *m(t)*,

$$m(t) = \left(M(SO_2)\beta + \frac{\gamma\beta}{\alpha}\right)t + \frac{\gamma\beta}{\alpha^2}(e^{-\alpha t}-1), \quad [14]$$

where

$$\alpha = k_1' + k_3a\sqrt{KP(O_2)}$$
$$\beta = k_1P(SO_2)$$
$$\gamma = M(O)k_3a\sqrt{KP(O_2)} - M(SO_2)k_1'.$$

The calculated expression [14] was compared to the experimental curves of weight variation versus time. Figure 6 illustrates the fitted curves obtained for two partial pressure

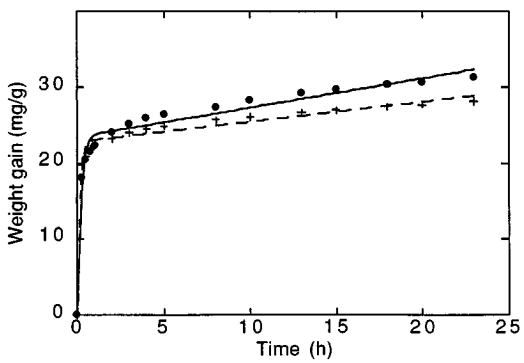

FIG. 6. Comparison between the experimental variation of the weight versus time and the theoretical curve (— or – – –) given by the *m(t)* expression of the kinetic model for two experiments. • $P(SO_2)$ = 0.8 kPa; $P(O_2)$ = 14.6 kPa; + $P(SO_2)$ = 0.8 kPa; $P(O_2)$ = 3.3 kPa.

conditions. We then have α, β, and γ values for all the experiments and this allows us to determine k_1, k'_1, and $ak_3\sqrt{K}$ (Table 3). However, it is not possible to separate k_3 from K and a. The averaged values of k_1, k'_1 and $ak_3\sqrt{K}$ from the results of Table 3 are

$$k_1 = 2.6\times10^{-6}\ \text{Pa}^{-1}\ \text{h}^{-1}\ \text{molg}^{-1}$$
$$k_1' = 7.7\ \text{h}^{-1}$$
$$ak_3\sqrt{K} = 1.6\times10^{-4}\ \text{Pa}^{-1/2}\ \text{h}^{-1}$$

We check that $ak_3\sqrt{KP(O_2)}$ is negligible compared with k'_1. To confirm these results, a kinetic model for SO_2 adsorption is proposed:

$$SO_2 + O^x_{Osurf} \leftrightarrows SO^x_{3Osurf}.$$

Just as for the sulfation model, we take into account the two reactions of adsorption and desorption of SO_2. Using the same approximations and notation as in the sulfation model, we write the following expression for *dm/dt*:

$$\frac{dm}{dt} = 64k_1P(SO_2) - 64k_1'[SO^x_{3Osurf}]. \quad [15]$$

The rate of variation of the amount of SO^x_{3Osurf} species is

$$\frac{d[SO^x_{3O}]}{dt} = k_1P(SO_2) - k_1'[SO^x_{3Osurf}], \quad [16]$$

and by integration we obtain the concentration versus time

$$[SO^x_{3Osurf}] = \frac{k_1P(SO_2)}{k_1'}(1-e^{-k_1't}). \quad [17]$$

The $[SO^x_{3Osurf}]$ and *dm/dt* limits are

$$[SO^x_{3Osurf}](t\to0) = 0 \quad \text{then } \frac{dm}{dt}(t\to0) = 64k_1P(SO_2) \quad [18]$$

$$[SO^x_{3Osurf}](t\to\infty) = \frac{k_1P(SO_2)}{k_1'} \quad \text{then } \frac{dm}{dt}(t\to\infty) = 0. \quad [19]$$

The last condition is experimentally confirmed if we notice (see Fig. 1) that between the 18th and 24th hour there was no gain of mass. We thus integrate Eq. [16], which is

$$\frac{dm}{dt} = 64k_1P(SO_2)e^{-k_1't},$$

taking account of [17] to find the calculated expression of *m(t)*:

$$m(t) = \frac{64k_1P(SO_2)}{k_1'}(1-e^{-k_1't}). \quad [20]$$

TABLE 3

Evaluation of the Model Constants from Various Experiments

Experiment	$P(SO_2)$ (Pa)	$P(O_2)$ (Pa)	$k_1 \times 10^6$ ($Pa^{-1}h^{-1}$ mol g^{-1})	k_1' (h^{-1})	$ak_3\sqrt{K} \times 10^7$ $Pa^{-1/2}h^{-1}$
1	800	200	3.2	7.4	4.7
2		360	3.8	8.4	3.4
3		560	1.4	3.3	0.9
4		820	3.5	7.6	1.9
5		1820	5.9	8.3	1.6
6		3210	3.1	7.3	0.8
7		6690	1.1	1.9	1.5
8		10745	3.4	7.2	1.4
9		14500	2.3	5.0	1.1
10	2660	3210	1.3	7.4	1.8
11	5320		0.8	8.5	1.3
12	7980		0.4	7.3	2.1

This expression enables us to find the shape of the experimental curve obtained from SO_2 adsorption on alumina at 350°C. We then find

$$k_1 = 2.9 \times 10^{-6}\ \text{Pa}^{-1}\ \text{h}^{-1}\ \text{mol g}^{-1}$$

$$k_1' = 7.0\,\text{h}^{-1}.$$

These values are similar to those obtained from the sulfation model. It therefore appears that the proposed model gives an account of the alumina sulfation mechanism by SO_2 oxidation in the absence of water.

CONCLUSION

Using thermogravimetric and infrared results, we propose a kinetic model for SO_2 adsorption and alumina sulfation by O_2 and SO_2. The elementary steps of the model of sulfation involve two types of sites. One is an oxygen atom of the alumina surface which contributes to the formation of sulfite or sulfate species depending on the absence or presence of oxygen. Under water pressure its role could be fulfilled by OH groups. Another site (present in a very low amount) is necessary to account for the dissociation of the oxygen molecules. A satisfactory agreement is obtained between the experimental curves of weight variation versus time and those deduced from the model. Moreover, the influence of the partial pressures of SO_2 and O_2 is that predicted by the model, which confirms its validity.

REFERENCES

1. Graulier, M., and Papee, D., *Energy Process. Can.* 1 (1974).
2. Quet, C., Tellier, J., and Voirin, R., *Stud. Surf. Sci. Catal.* **6**, 323 (1980).
3. Pearson, M., "38th Canadian Chemical Engineering Conference: Acid Gas Poisoning and Sulfur Recovery." Alberta, 1988.
4. Saussey, H., Vallet, A., and Lavalley, J. C., *Mater. Chem. Phys.* **9**, 457 (1983).
5. Nam, S. W., and Gavalas, G. R., *Appl. Catal.* **55**, 193 (1989).
6. Chang, C., *J. Catal.* **53**, 374 (1978).
7. Karge, H. G., and Dalla Lana, I. G., *J. Phys. Chem.* **88**, 1538 (1984).
8. Lavalley, J. C., Janin, A., and Preud'homme, J., *React. Kinet. Catal. Lett.* **18**, 85 (1981).
9. Datta, A., Cavell, R., Tower, R., and George, Z., *J. Phys. Chem.* **89**, 443 (1985).
10. Preud'homme, J., Lamotte, J., Janin, A., and Lavalley, J. C., *Bull. Soc. Chim. France* I-443 (1981).
11. Saur, O., Bensitel, M., Saad Mohammed, A. B., Lavalley, J. C., Tripp, C. P., and Morrow, B. A., *J. Catal.* **99**, 104 (1986).
12. Kröger, F. A., *in* "The Chemistry of Imperfect Crystals" 2nd ed. North-Holland, Amsterdam, 1974.